Langmuir

Article

pubs.acs.org/Langmuir

Surface-Controlled Properties of Myosin Studied by Electric Field Modulation

Harm van Zalinge,[†] Laurence C. Ramsey,[†] Jenny Aveyard,[†] Malin Persson,[‡] Alf Mansson,[‡] and Dan V. Nicolau*[,†,§]

[†]Department of Electrical Engineering & Electronics, University of Liverpool, L69 3GJ Liverpool, United Kingdom

[‡]Department of Chemistry and Biomedical Sciences, Linnaeus University, 39182 Kalmar, Sweden

[§]Department of Bioengineering, McGill University, Montreal, H3A 0C3 Quebec, Canada

ABSTRACT: The efficiency of dynamic nanodevices using surface-immobilized protein molecular motors, which have been proposed for diagnostics, drug discovery, and biocomputation, critically depends on the ability to precisely control the motion of motor-propelled, individual cytoskeletal filaments transporting cargo to designated locations. The efficiency of these devices also critically depends on the proper function of the propelling motors, which is controlled by their interaction with the surfaces they are immobilized on. Here we use a microfluidic device to study how the motion of the motile elements, i.e., actin filaments propelled by heavy mero-myosin (HMM) motor fragments immobilized on various surfaces, is altered by the application of electrical loads generated by an external electric field with strengths ranging from 0 to 8 kVm^{-1}. Because the motility is intimately linked to the function of surface-immobilized motors, the study also showed how the adsorption properties of HMM on various surfaces, such as nitrocellulose (NC), trimethylclorosilane (TMCS), poly(methyl methacrylate) (PMMA), poly(*tert*-butyl methacrylate) (PtBMA), and poly(butyl methacrylate) (PBMA), can be characterized using an external field. It was found that at an electric field of 5 kVm^{-1} the force exerted on the filaments is sufficient to overcome the frictionlike resistive force of the inactive motors. It was also found that the effect of assisting electric fields on the relative increase in the sliding velocity was markedly higher for the TMCS-derivatized surface than for all other polymer-based surfaces. An explanation of this behavior, based on the molecular rigidity of the TMCS-on-glass surfaces as opposed to the flexibility of the polymer-based ones, is considered. To this end, the proposed microfluidic device could be used to select appropriate surfaces for future lab-on-a-chip applications as illustrated here for the almost ideal TMCS surface. Furthermore, the proposed methodology can be used to gain fundamental insights into the functioning of protein molecular motors, such as the force exerted by the motors under different operational conditions.

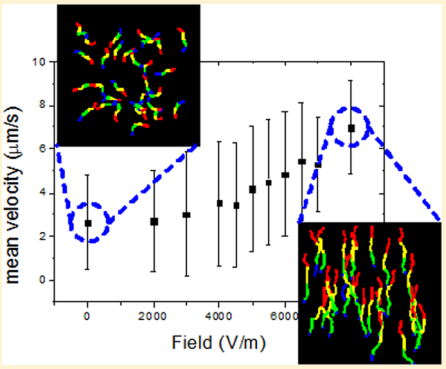

1. INTRODUCTION

Molecular motors are responsible for the generation of force and for motion at the nanometer scale in biological systems. Linear molecular motors, an essential class among these systems, comprise the subclasses of myosins,[1,2] kinesins,[3,4] and dyneins.[5] An example of force generation by molecular motors is muscle contraction, which is powered by the actin−myosin system through the ATP-fuelled translocation of actin filaments by myosin II motors.[6,7] The study of molecular-motor-induced motion and force generation in vitro was enabled by the development of the in vitro motility assay in the late 1980s, which allowed the visualization of the motility of either myosin-coated fluorescent beads moving over surface-bound actin filaments[8,9] or fluorescently labeled actin filaments moving over a layer of surface-bound myosin or its fragments, e.g., heavy meromyosin (HMM).[10] Because the latter architecture of the motility assay is considerably easier to implement, it has been used extensively for the study of the fundamentals of molecular motor function.[11−13]

Because the actin−myosin II motor system is critical to the functioning of both skeletal[14,15] and heart muscle,[16] this system has been comprehensively studied using in vitro motility assays and other techniques.[17,18] Recently, such studies have aided and continue to aid the development of acto-myosin active drugs, e.g., in the treatment of heart failure and cardiomyopathies.[18−20] These studies would also greatly benefit from experiments where external forces are exerted on the protein motor system, as opposed to the classical studies of unloaded motor proteins as performed in conventional in vitro motility assays.[21,22]

It has been reported previously that because of the negative charge of the actin filaments an electric force can be used to direct their motion in an in vitro motility assay.[23−25] The development of electric motility assays would open this classical technique to high-throughput, highly miniaturized studies,

Received: April 29, 2015
Revised: July 9, 2015
Published: July 10, 2015

DOI: 10.1021/acs.langmuir.5b01549
Langmuir 2015, 31, 8354−8361

which is important to the efficiency of drug discovery efforts[18,26] because specific myosins can be purified only in small amounts and at high costs, e.g., human myosin with and without myopathy mutations.[27,28] Furthermore, such electric motility lab-on-a-chip systems would provide important opportunities in molecular-motor-driven biocomputation[29] and diagnostics applications.[30] The advanced fundamental understanding of electrophoresis[24] and dielectrophoresis,[25] as well as of the nanomechanics of protein molecular motors,[31,32] and their surface adsorption[33,34] constitute an important basis for such developments. However, the inter-relationship among these three elements has not been thoroughly considered so far, thus delaying the development of assays where external electric forces are applied in molecular-motor-based nanodevices. In addition, there are other design criteria which have not been fully addressed, such as the user friendliness of the developed devices and the adaptability of the devices for high-throughput applications.

To this end, we propose a simple microfluidics device based on the application of tunable electrophoretic forces on motile actin filaments to demonstrate the control of the motility of cytoskeletal filaments and probe the impact of surfaces and electric external forces on the function of protein molecular motors using heavy meromyosin from skeletal muscle as a model system.

2. EXPERIMENTAL DETAILS

2.1. Chemicals and Surface Functionalization. All chemicals were purchased from Sigma-Aldrich unless otherwise stated and used as received. The solutions were prepared as follows: nitrocellulose (NC) 1% (w/v) in amyl acetate; poly(methyl methacrylate) (PMMA, average M_w = 120 000) 2% (w/v) in propylene glycol monomethyl ether acetate (PGMEA); poly(tertbutyl methacrylate) (PtBMA, average M_w = 170 000) 2% (w/v) in PGMEA; poly(butyl methacrylate) (PBMA, average M_w = 180 000; Polysciences Europe) 1% (w/v) in toluene. Trimethylchlorosilane (TMCS) 5% in chloroform was also used.

The coverslips used to build the flow cell were functionalized prior to device assembly. For polymer functionalization, glass coverslips were rinsed in ethanol and dried under a nitrogen flow before they were spin coated with the polymer solutions at 3600 rpm for 2 min. The coverslips were then baked at 85 °C for 3 h.

For TMCS functionalization, glass coverslips were soaked in dry acetone, methanol, and chloroform for 5 min each. The surface treatment is aimed at removing organic contaminants while we rely on the presence of surface silanol groups on glass surfaces under ambient conditions for silanization.[5] This is rather similar to the approach used by Sundberg et al.,[35] giving TMCS-derivatized surfaces with similar contact angles as in the present work. The coverslips were then soaked in TMCS for 5 min.[35] After silanization, coverslips were rinsed in dry chloroform, dried under a flow of nitrogen, and subsequently baked at 85 °C for 1 h.

The following solutions were used for in vitro motility assays: (1) Low ionic strength solution (LISS), 1 mM $MgCl_2$, 10 mM MOPS, 0.1 mM K_2EGTA, pH 7.4. (2) B65, LISS containing 50 mM KCl and 10 mM dithiothreitol (DTT). (3.) Assay solution, 1 mM MgATP, 10 mM DTT, 25 mM KCl, and LISS with an antibleach mixture containing 3 mg/mL^{-1} glucose, 20 units/mL glucose oxidase, 870 units/mL catalase, and an ATP regenerating system containing 2.5 mM creatine phosphate and 56 units/mL creatine kinase. (4) Blocking solution: 1 mg mL^{-1} bovine serum albumin (BSA) in LISS buffer. (5) Labeled actin: 10 μL of rhodamine phalloidin-labeled actin filaments (rhodamine phalloidin was purchased from Invitrogen and actin was labeled according to the manufacturer's protocol) in 990 μL of B65. (6) Blocking actin solution, 14 μL of unlabeled actin filaments, 986 μL of B65.

2.2. Motility Assay. The motility experiments were performed in the following sequence. First 60 μL of heavy meromyosin (HMM; 120 μg/mL in B65) was applied to a flow cell containing the functionalized coverslip and incubated for 2 min. At the end of this period, unoccupied binding sites on the coverslip were blocked by applying 60 μL of blocking solution to the flow cell. Following incubation for 30 s, the blocking solution in the flow cell was replaced with 60 μL of blocking actin (to block nonfunctioning HMM heads). After 1 min of incubation, excess blocking actin was removed by flushing the flow cell with 60 μL of B65, and then 60 μL of labeled actin was applied for 30 s. At the end of this time period, excess labeled actin was removed by flushing the flow cell with 60 μL of B65, and 60 μL of an assay solution was applied.

2.3. Electric Motility Flow Cell. The electric field was applied to the motility assay in a cell as shown in Figure 1. The motility of actin filaments occurs on glass coverslips functionalized as described above. These coverslips were attached to a microscope slide via thin spacers.[10] Tall plastic cones, modified from pipet tips to hold copper electrodes at the top, were sealed at the open edges of the flow cell.

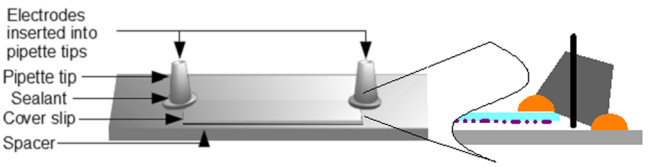

Figure 1. Device setup for the electrical motility assay. The spacer creates space between the glass slide and the coverslip. The inset to the right is a cross section of the device at the electrode end, showing its position in the flow cell.

2.4. Visualization of Motility. The movement of the filaments was studied using an epifluorescence microscope (Zeiss Axio Imager.M1) fitted with an Andor iXon+ EMCCD camera at room temperature. Videos were acquired at a frame rate of 10 frames s^{-1}. The analysis of the videos was performed using open source image-processing program imageJ,[36] and the filament movement was tracked using plugin MtrackJ. The velocity of the filaments was characterized by the change in position of the leading end of the filament from frame to frame, while the angle of the movement was determined relative to the direction of the positive electrode. Only the filaments that were fully motile for the entire 50 frames of a video were tracked. The average filament length for all experiments was (1.0 ± 0.1) μm (mean ± standard deviation). The average velocity as reported in this article is defined as the velocity from frame to frame for 30 individual filaments.

2.5. Electric Field. During the motility experiments, the electrical field was varied between 0 and 8 kVm^{-1}. The electric field affects the movement of the actin filament because of its negative, linearly distributed charge which is recorded as being approximately 4 e$^-$ nm^{-1}, with e$^-$ being the electron charge, -1.6×10^{-19} C, with a surface charge density of 0.15 e$^-$ nm^{-2}.[37,38]

During the experiments the ambient temperature of the flow cell stayed within ±0.2 °C of its mean value, and thus it can be concluded that the velocity of actin filaments was not influenced by variations of temperature inside the flow cell.[39]

3. RESULTS

3.1. Electrically Controlled Motility on Nitrocellulose. Because of the negative charge of the actin filaments (pI 5.4),[40] the application of an electric field translates into an increase in the apparent velocity of the movement and its guidance toward the positive electrode (Figure 2, right inset). As also observed by others,[23,24] some filaments initially moved toward the negative electrode, but in our study the lack of lateral confinement of the motion of the actin filaments coupled with the nearly random movement of the actin filament leading

DOI: 10.1021/acs.langmuir.5b01549
Langmuir 2015, 31, 8354−8361

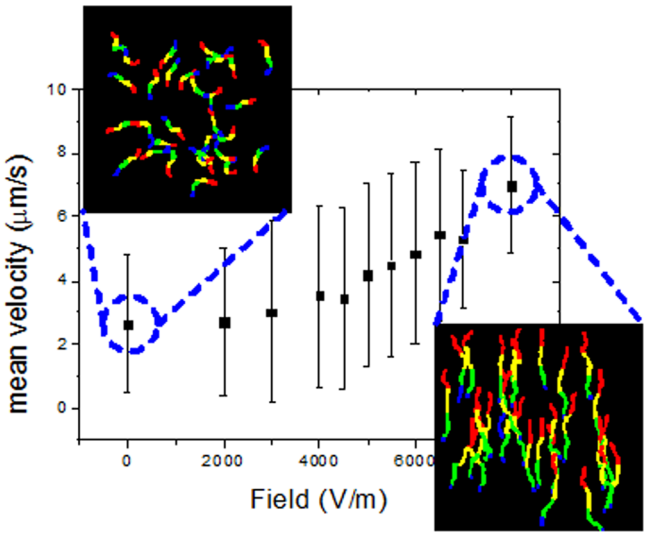

Figure 2. Average sliding velocity of actin filaments, in absolute value, as a function of the electric field on a HMM-functionalized nitrocellulose surface. The error bars indicate one standard deviation. The insets present the trajectories of actin filaments (n = 30) at the indicated electric fields: left, at zero electric field; right, at 8 kVm^{-1}. The movement starts at the red end and finishes at the blue end. All experiments were performed at a constant room temperature of 22−23 °C.

ends resulted in them quickly making U-turns, followed by movement toward the positive electrode.

Figure 2 presents the absolute value of the sliding velocity of the actin filaments as a function of the strength of the electrical field when the filaments were propelled by HMM immobilized on a nitrocellulose surface. The slope of the velocity vs field strength plot shows a transition regime starting at 5 kVm^{-1}, above which there is a substantial increase in the slope. Although the force generated by the electric field rises linearly with the field strength, the response of the actin filaments becomes nonlinear due to the various forces that act on the filament; for example, the resistive motors will resist motility toward the positive electrode.

Apart from the increase in sliding velocity, the application of an electric field also affected the motion directionality, as can be observed from the two insets in Figure 2. At electric fields close to zero the filaments move randomly, but once the field increases the filaments start to move toward the positive electrode. At the maximum applied field of 8 kV m^{-1} there are no recorded movements toward the negative electrode (inset in Figure 2).

3.2. Electrical Motility on Different Surfaces. To be able to study how the binding of the myosin to the surface and thus the motility are affected by the surface properties, various surface functionalizations were used. An overview of these and some of their key properties are listed in Table 1.

In principle, the electric force applied to actin filaments could result from electrophoresis, dielectrophoresis, or electrosmotic flow phenomena. However, the largely symmetric nature of the system involved, i.e., the surface, effectively rules out dielectrophoresis, and the electrically heterogeneous nature of the protein-functionalized surface, which is deleterious to the formation of a contiguous electric double layer, rules out electroosmotic flow. Consequently, the largest contributor to electrical motility is the electrophoretic forces applied to negatively charged actin filaments.[23−25]

The general, relationships between the average velocity of the actin filaments and the strength of the electric fields were similar for different HMM-immobilizing surfaces (Figure 3),

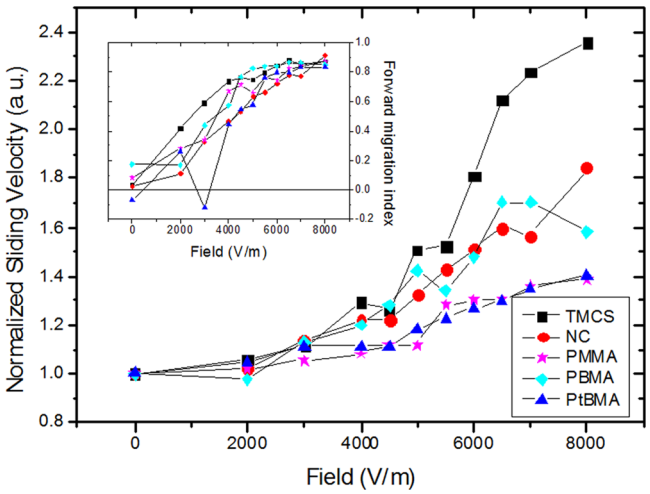

Figure 3. Average sliding velocity of actin filaments propelled by HMM immobilized on different surfaces, normalized with respect to the zero field velocity. Each velocity point is an average of 1500 recorded movements of filaments. The standard deviation of the velocities (error bars not included for clarity) was less than ±1.5. The inset shows the forward migration index. All experiments have been performed at constant room temperature.

i.e., the sliding velocity increased with the increased electric field strengths, with a change in slope at approximately 5 kV m^{-1}. Similarly, the direction of travel of the filaments changed from random to a parallel motion along the electric field axis as the field strength increased (Table 1). This is highlighted by the

Table 1. Contact Angle and Actin Filament Motility Characteristics at Different Electric Field Strengths for the Various Surfaces Used to Immobilize HMM

		electric field					
		4 kVm^{-1}		6 kVm^{-1}		8 kVm^{-1}	
surface	contact angle	filaments moving within ±20° of field axis (%)	motile filaments (%)	filaments moving within ±20° of field axis (%)	motile filaments (%)	filaments moving within ±20° of field axis (%)	motile filaments (%)
PMMA	61.5 ± 0.6	47.1 ± 0.6	42.1 ± 4	48.6 ± 0.6	46.3 ± 4	64.3 ± 0.6	60.3 ± 4
NC	70.1 ± 0.6	35.5 ± 0.6	30.6 ± 4	47.8 ± 0.6	34.3 ± 4	74.9 ± 0.6	66.9 ± 4
TMCS	71.0 ± 0.6	59.6 ± 0.6	38.7 ± 4	63.9 ± 0.6	44.4 ± 4	66.0 ± 0.6	80.5 ± 4
PtBMA	80.1 ± 0.6	40.0 ± 0.6	31.9 ± 4	58.7 ± 0.6	33.8 ± 4	60.7 ± 0.6	51.6 ± 4
PBMA	80.9 ± 0.6	41.4 ± 0.6	25.0 ± 4	64.6 ± 0.6	27.1 ± 4	65.3 ± 0.6	42.0 ± 4

DOI: 10.1021/acs.langmuir.5b01549
Langmuir 2015, 31, 8354−8361

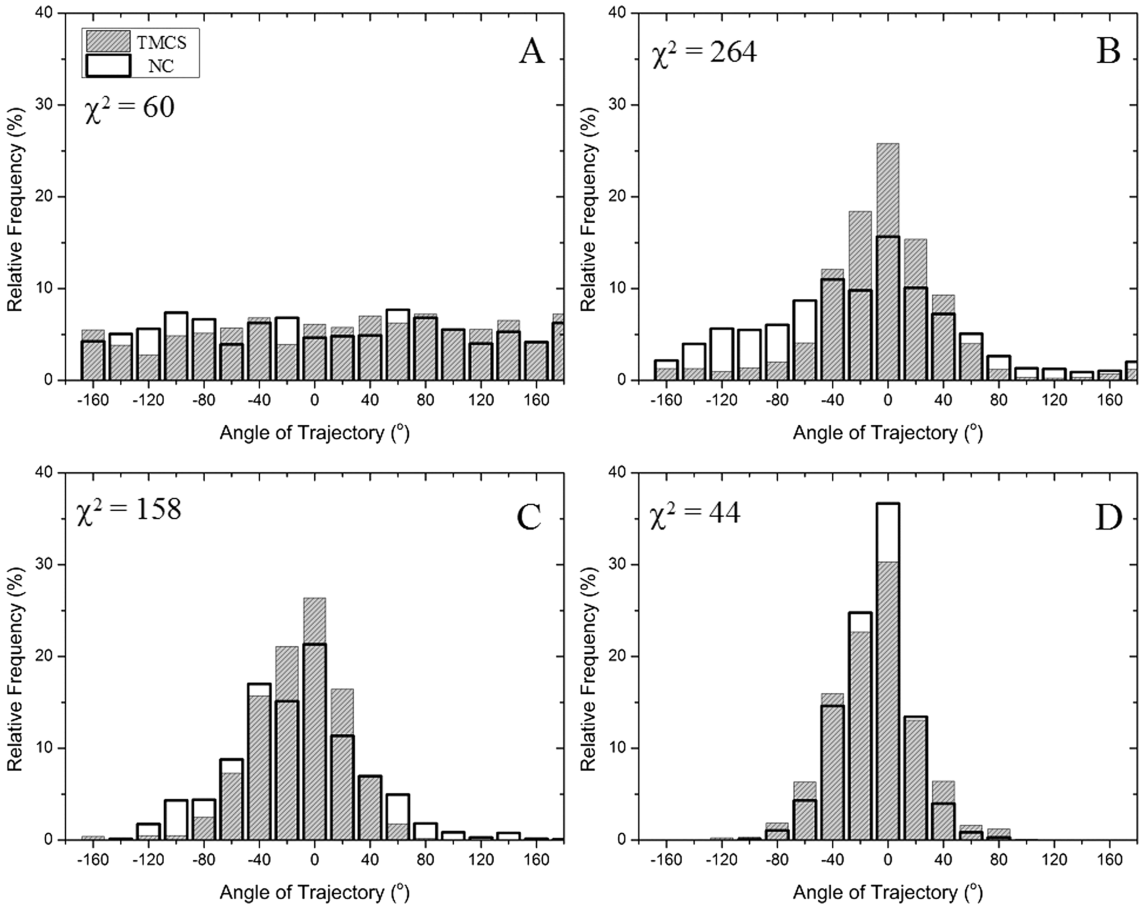

Figure 4. Distribution of angular sliding directions of actin filaments on model surfaces, i.e., NC and TMCS. 0° represents the axis of the electric field. (A) No field applied, (B) 4 kV/m, (C) 6 kV/m, and (D) 8 kV/m. The χ^2 values compare the distribution on TMCS with that on NC.

inset of Figure 3 in which the forward migration index (FMI) of the experiments is shown. The FMI represents the efficiency of the movement in a particular direction, in this case, the actin filament toward the positive electrode. The FMI is defined as

$$x_{\mathrm{FMI}} = \frac{1}{n}\sum_{i=1}^{n}\frac{x_i}{d_i} \tag{1}$$

where n represents the number of steps, or frames, of the filament movement; x represents the component of the movement of the filament toward the positive electrode, and d represents the total movement of the filament, both of which are taken between two subsequent frames. All of the effects caused by the electric field were reversible.

The directionality of motion, studied in detail for TMCS and nitrocellulose surfaces (Figure 4), presents similar characteristics, i.e., increased propensity of alignment of the motion along the electric field with increased field strength. The χ^2 value between the angular distribution on TMCS and NC, which estimates the overlap between the two distributions, shows that the directionality of the filaments on NC and TMCS was very similar at low and high strengths of the electric fields.

4. DISCUSSION

4.1. Forces Exerted on the Actin Filament. For surfaces with a contact angle in the range 60−80°, as in the present study (Table 1), the HMM molecules adsorb preferentially via their C-terminal tail domain with the N-terminal motor domain extending into solution.[21] Despite this favorable molecular positioning, an essential feature of nonprocessive motors, such as myosin II, is that a fraction of the motors interacting with the actin filaments are pushing in the direction of the actual movement while another fraction of the motors opposes this movement, thus effectively creating a resistive force.[41,42] These resistive motors, which do not contribute to motion, comprise both motors that oppose any motility by holding the filament (e.g., ATP-insensitive rigor-like motors) as well as those that are simply "pushing" in another direction than that of the actual movement, i.e., when they are moved into a drag stroke region by the active motors.[42,43] The actual ratio of the active and resistive motors is governed by experimental parameters, e.g., the ratio of active vs total protein molecules, which is the result of different preparation protocols, or the level of denaturation of the motor protein in contact with different immobilizing surfaces. When a measurable, controllable, and external additional force, e.g., a force generated by an electric field, is applied to this tug-of-war nanomechanical system, the natural equilibrium between internal forces will be biased. The new steady-state will be reached as a result of the new equilibrium between the external force and the overall internal force, where the latter is determined by the total number of actomyosin cross-bridges and the average elastic strain energy in each cross-bridge. Therefore, the application of different loads on the actin filaments will be associated with differing actomyosin interaction kinetics, thus allowing the probing of a wider spectrum of the strain dependence of the chemomechanical

DOI: 10.1021/acs.langmuir.5b01549
Langmuir 2015, 31, 8354−8361

coupling. This is the central principle of the electric motility experiments.

4.2. Impact of Surface Molecular Rigidity on Motility. Key properties of the surfaces that impact the surface-immobilized proteins are surface hydrophobicity, charging, and molecular rigidity.[44,45] These properties impact the immobilization and function of HMM, as has experimentally been verified for surface hydrophobicity,[33,46] its molecular rigidity,[47] and its charge.[33] While these parameters are interlinked to some extent and additional effects might play a role in the determination of the motility function, a selection of surfaces that have similar parameters except for one would allow the assessment of that single parameter. Because NC and TMCS surfaces have very similar hydrophobicity (Table 1) and both are negatively charged, the remaining and important difference is their molecular rigidity.[33,48] Indeed, the TMCS-functionalized glass will not absorb water, thus conserving its rigidity, whereas the polymer nature of NC will allow the uptake of water and build a gel-like thin layer on top of the surface. Consequently, the anchoring points for the myosin motors are located on a flat plane on TMCS surfaces, but the motor proteins will be partially embedded in the hydrated top NC polymer. Figure 5 presents a schematic of the proposed

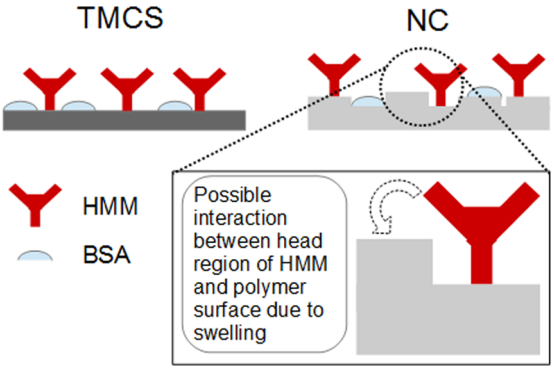

Figure 5. Different architectures of an HMM-immobilizing surface on rigid, e.g., TMCS, surfaces and top-swelled polymeric, e.g., NC, surfaces.

mechanisms for HMM immobilization on TMCS and NS surfaces. As opposed to TMCS surfaces, the top polymer chains on NC surfaces can interact with several regions of the bound HMM molecules, including the motor domains (heads), thereby potentially hindering motility.[47]

However, the similarity in the motility behavior on NC and TMCS in the absence of an electric field (Figure 3) suggests that any difference in the binding characteristics of the two surfaces is rather small when external forces are not exerted on the actin filaments. Indeed, this is in agreement with previous findings showing that the adsorption of HMM and blocking protein prior to the actual motility assay result in a protein layer which decreases the difference between the overall rigidity of the NC and TMCS surfaces.[47] The coating of surfaces with NC[10,12,49] and the functionalization with TMCS[33,43] have been used extensively as immobilizing surfaces for HMM in studies of motor protein function. Both of these surface substrates are relativity hydrophobic, and it has been shown in numerous motility studies that both TMCS and NC exhibit fully functioning myosin motors.[22,46,50−53]

While the actin filament sliding velocity was very similar on NC and TMCS surfaces in the absence of an electric field (Figure 3), it was only when a substantial field was applied that the motility behavior differed between the two surfaces. In particular, the motility appeared to be less hindered on TMCS than on NC, as inferred by the larger increase in the velocity on these surfaces when the electric fields strength increases from 0 to 8 kVm^{-1}. In the framework of the proposed model of the interaction between HMM and the immobilizing surface, it appears that the more exposed protein architecture on TMCS-functionalized surfaces allows a more direct and thus a more effective interaction with the electric fields than on the more embedded architecture on NC surfaces. This finding is consistent with better (higher velocity and larger fraction of motile filaments) and more reproducible motility previously observed on TMCS-derivatized surfaces compared to NC surfaces.[35,54]

4.3. Impact of Surface Hydrophobicity on Motility. To examine the effect of hydrophobicity, the motility on a range of polymer coatings (PtBMA, PBMA, and PMMA) was compared to the motility on NC. In contrast to NC and TMCS, polymers PtBMA and PBMA are not commonly used as a substrates for protein immobilization, but they have, as well as PMMA,[46,54,55] been shown to support actin myosin motility.[22] Among these polymers, PMMA is relatively hydrophilic (Table 1). It differs from PtBMA and PBMA in the end ester group linked to the methacrylic backbone polymeric chain. Therefore, any changes in the HMM immobilization-induced properties of the surface are due to the chemical characteristics and not the structural properties.

One property which distinguishes the motility function of the various surfaces is the steep increase in the average sliding velocity of actin filaments in the midrange (4.5−6 kV m^{-1}) upon further increases in electric field strength (Figure 3).[24] Interestingly, the behavior is consistent with observations in living muscle cells that are subjected to an assisting load due to parallel elastic elements.[56,57] When looking at the information obtained from the directionality of the filament movement as shown in Figure 4 and Table 1, the main observation is that the degree of directionality increases in parallel with the increase in velocity. When the electric field was switched on, the negatively charged filaments responded to the force generated by the field and moved toward the positive electrode (0°). In general, at 5 kV m^{-1}, all filaments on the various substrates moved within ±90° from the positive electrode, changing to ±40° at the maximum field of 8 kVm^{-1}.

The fact that the increase in sliding velocity as a function of electric field, the directionality, and the percentage of motile filaments all occur at 5 kV m^{-1} gives possible insight into its cause. While the motility function is determined by the ability of the apex of the filament to find the next molecular motor, this is complicated by the fact that the motors have a preferential direction in which they propel the filaments and the presence of "dead" motors which resist motion completely. If the force generated by the electric field at the threshold value of 5 kV m^{-1} is similar to the force generated by the resistive motors, then at higher field strengths more filaments, which were blocked by these motors, will start to move, and thus an increase in the percentage of motile filaments will be observed. While at low fields the direction of the apex of the actin filament is governed by Brownian motion, as the strength of the field is increased, the movement of the apex is forced toward the positive electrode, resulting in the apex finding fewer motors in its path. Additionally, the longer time span between the attachment of the apex to subsequent motors allows the

DOI: 10.1021/acs.langmuir.5b01549
Langmuir 2015, 31, 8354−8361

field to transfer more force onto the filament, and hence an increased acceleration can be observed.

The exceptional behavior of motility on TMCS is of particular interest because several studies have shown that this surface provides a better HMM function than other substrates to which it has been compared.[21,33,35] This behavior has been explained by the predominant adsorption of HMM motor fragments via their most C-terminal tail domain to a TMCS-functionalized surface. Such an adsorption mechanism, with the myosin heads more than 30 nm from the surface,[21] has been attributed to the moderate hydrophobicity of TMCS and a low negative electric charge density, partially repelling the HMM C-terminal.[21,33,35] This mode of adsorption would make the subfragment 2 (S2) tail fragment of actin-attached HMM amenable to buckling when subjected to assistive forces acting in the same direction as the motor-driven filament sliding.[58,59] Such properties seem to be consistent with a substantial increase in velocity with increased assisting loads, e.g., due to electric fields, because the S2 fragments of actin-attached HMM give minimal internal resistance to sliding. The difference between TMCS and the other substrates in the velocity versus field-strength plots may be due to the lack of S2 buckling on the latter substrates. This could be the result if negatively charged subfragment 2 or one of the myosin heads (Figure 5) is bound to the underlying surface in the polymer substrates because of either increased surface roughness or specific chemical properties.

4.4. On the Design of a Future High-Throughput Electric Motility Assay. The overall design of the motility chamber in the present study is built on the standard design of flow cells in conventional motility assays.[10] In spite of the simplicity of the design, the chambers that house the electrodes are contained and separated from the actual motility chamber. This is important, both for preventing the deterioration of imaging by microbubbles and to ensure the separation of motors from the motility-toxic chemical species created during electrolysis, e.g., hydrogen, oxygen, and radicals. Equally important, this design results in the establishment of essentially parallel electric field lines, thus creating an area where all filaments and motors experience a similar electrophoretic force in both amplitude and direction.

In future electric motility lab-on-a-chip devices, whether for drug discovery, diagnostics, or biocomputation, it will be important to select an appropriate surface substrate for the adsorption of motor fragments. Particularly important for the fundamental studies and those focused on drug discovery is that it is important to consider the fact that the myosin motor fragments have different properties on different substrates, as shown above. We have shown that motility is of good quality on both NC and TMCS as well as on PMMA. Out of these substrates, TMCS and NC have advantages by virtue of the long technological experience and careful characterization of HMM function, whereas PMMA is a material widely used in the fabrication of microfluidic devices. A disadvantage of NC, not present for PMMA and TMCS, is that it is not readily micro- or nanopatterned, which may be important in certain applications requiring the confinement of the movement of actin filaments.

5. CONCLUSIONS

We have studied how the motion of actin filaments, which are propelled by heavy mero-myosin (HMM) motor fragments adsorbed to different surface substrates, is altered by the application of loads created by electric fields. We demonstrated how the proposed devices can be used for the selection of motility-friendly surfaces, which is a critical design element for future prototypes of nanodevices based on the use of protein molecular motors. In addition, the application of external forces provides an important tool for gathering more insight into the adsorption mechanism of HMM and how it depends on the physical properties of the adsorbing surface. In particular, we found that the effect of assisting electric fields on the relative increase in the sliding velocity was markedly higher for TMCS than for any other surfaces tested, with implications for the design of future high-throughput electric motility assays. The directionality of the motility was observed to be different at intermediate field strengths but similar at the high and low fields when comparing rigid and nonrigid surfaces.

AUTHOR INFORMATION

Corresponding Author

*E-mail: dan.nicolau@mcgill.ca.

Author Contributions

The manuscript was written through the contributions of all authors. All authors have given approval to the final version of the manuscript. H.v.Z. and L.C.R. contributed equally.

Funding

We acknowledge funding from the European Union Seventh Framework Programme ([FP7/2007−2011]) under grant agreement number 228971 (MONAD) and from the Swedish Research Council (grant no. 621-2010-5146).

Notes

The authors declare no competing financial interest.

REFERENCES

(1) Sellers, J. R.; Veigel, C. Walking with myosin V. *Curr. Opin. Cell Biol.* **2006**, *18* (1), 68−73.

(2) Sweeney, H. L.; Houdusse, A. Structural and functional insights into the myosin motor mechanism. *Annu. Rev. Biophys.* **2010**, *39*, 539−557.

(3) Block, S. M. Kinesin motor mechanics: Binding, stepping, tracking, gating, and limping. *Biophys. J.* **2007**, *92* (9), 2986−2995.

(4) Hirokawa, N.; Noda, Y.; Tanaka, Y.; Niwa, S. Kinesin superfamily motor proteins and intracellular transport. *Nat. Rev. Mol. Cell Biol.* **2009**, *10* (10), 682−696.

(5) McIntire, T. M.; Smalley, S. R.; Newberg, J. T.; Lea, A. S.; Hemminger, J. C.; Finlayson-Pitts, B. J. Substrate changes associated with the chemistry of self-assembled monolayers on silicon. *Langmuir* **2006**, *22* (13), 5617−5624.

(6) Huxley, A. F.; Niedergerke, R. Structural change in muscle during contraction - interference microscopy of living muscle fibres. *Nature* **1954**, *173* (4412), 971−973.

(7) Huxley, H.; Hanson, J. Changes in the cross-striations of muscle during contraction and strech and their structural interpretation. *Nature* **1954**, *173* (4412), 973−976.

(8) Sheetz, M. P.; Spudich, J. A. Movement of Myosin-Coated Fluorescent Beads on Actin Cables Invitro. *Nature* **1983**, *303* (5912), 31−35.

(9) Spudich, J. A.; Kron, S. J.; Sheetz, M. P. Movement of myosin-coated beads on oriented filaments reconstituted from purified actin. *Nature* **1985**, *315* (6020), 584−586.

(10) Kron, S. J.; Spudich, J. A. Fluorescent actin filaments move on myosin fixed to a glass surface. *Proc. Natl. Acad. Sci. U. S. A.* **1986**, *83* (17), 6272−6276.

(11) Harada, Y.; Noguchi, A.; Kishino, A.; Yanagida, T. Sliding movement of single actin filaments on one-headed myosin filaments. *Nature* **1987**, *326* (6115), 805−808.

DOI: 10.1021/acs.langmuir.5b01549
Langmuir 2015, 31, 8354−8361

(12) Toyoshima, Y. Y.; Kron, S. J.; Spudich, J. A. The myosin step size: measurement of the unit displacement per ATP hydrolyzed in an *in vitro* assay. *Proc. Natl. Acad. Sci. U. S. A.* **1990**, *87*, 7130−7134.
(13) Uyeda, T. Q. P.; Abramson, P. D.; Spudich, J. A. The neck region of the myosin motor domain acts as a lever arm to generate movement. *Proc. Natl. Acad. Sci. U. S. A.* **1996**, *93* (9), 4459−4464.
(14) Spudich, J. A.; Huxley, H. E.; Finch, J. T. Regulation of skeletal muscle contraction. II. Structural studies of the interaction of the tropomyosin-troponin complex with actin. *J. Mol. Biol.* **1972**, *72* (3), 619−632.
(15) Spudich, J. A.; Watt, S. The regulation of rabbit skeletal muscle contraction. I. Biochemical studies of the interaction of the tropomyosin-troponin complex with actin and the proteolytic fragments of myosin. *J. Biol. Chem.* **1971**, *246* (15), 4866−4871.
(16) Alpert, N. R.; Hamrell, B. B.; Mulieri, L. A. Heart muscle mechanics. *Annu. Rev. Physiol.* **1979**, *41*, 521−537.
(17) Behrmann, E.; Müller, M.; Penczek, P. A.; Mannherz, H. G.; Manstein, D. J.; Raunser, S. Structure of the rigor actin-tropomyosin-myosin complex. *Cell* **2012**, *150* (2), 327−338.
(18) Spudich, J. A. Hypertrophic and dilated cardiomyopathy: Four decades of basic research on muscle lead to potential therapeutic approaches to these devastating genetic diseases. *Biophys. J.* **2014**, *106* (6), 1236−1249.
(19) Cleland, J. G. F.; Teerlink, J. R.; Senior, R.; Nifontov, E. M.; McMurray, J. J. V.; Lang, C. C.; Tsyrlin, V. A.; Greenberg, B. H.; Mayet, J.; Francis, D. P.; Shaburishvili, T.; Monaghan, M.; Saltzberg, M.; Neyses, L.; Wasserman, S. M.; Lee, J. H.; Saikali, K. G.; Clarke, C. P.; Goldman, J. H.; Wolff, A. A.; Malik, F. I. The effects of the cardiac myosin activator, omecamtiv mecarbil, on cardiac function in systolic heart failure: A double-blind, placebo-controlled, crossover, dose-ranging phase 2 trial. *Lancet* **2011**, *378* (9792), 676−683.
(20) Fedorov, R.; Böhl, M.; Tsiavaliaris, G.; Hartmann, F. K.; Taft, M. H.; Baruch, P.; Brenner, B.; Martin, R.; Knölker, H. J.; Gutzeit, H. O.; Manstein, D. J. The mechanism of pentabromopseudilin inhibition of myosin motor activity. *Nat. Struct. Mol. Biol.* **2009**, *16* (1), 80−88.
(21) Persson, M.; Albet-Torres, N.; Ionov, L.; Sundberg, M.; Hook, F.; Diez, S.; Mansson, A.; Balaz, M. Heavy Meromyosin Molecules Extending More Than 50 nm above Adsorbing Electronegative Surfaces. *Langmuir* **2010**, *26* (12), 9927−9936.
(22) Hanson, K. L.; Solana, G.; Nicolau, D. V. Effect of Surface Chemistry on in Vitro Actomyosin Motility. In *Biomedical Applications of Micro- and Nanoengineering II*; Nicolau, D. V., Ed.; SPIE: Bellingham, WA, 2005; Vol. *5651*, pp 13−18.
(23) Hanson, K. L.; Solana, G.; Nicolau, D. V. Electrophoretic control of actomyosin motility. *Proc. SPIE* **2005**, *5699*, 196−201.
(24) Riveline, D.; Ott, A.; Julicher, F.; Winkelmann, D. A.; Cardoso, O.; Lacapere, J. J.; Magnusdottir, S.; Viovy, J. L.; Gorre-Talini, L.; Prost, J. Acting on actin: the electric motility assay. *Eur. Biophys. J.* **1998**, *27* (4), 403−408.
(25) van den Heuvel, M. G. L.; Butcher, C. T.; Lemay, S. G.; Diez, S.; Dekker, C. Electrical docking of microtubules for kinesin-driven motility in nanostructures. *Nano Lett.* **2005**, *5* (2), 235−241.
(26) McMurray, J. J. V. Heart failure in 2011: Heart failure therapyĝ€″technology to the fore. *Nat. Rev. Cardiol.* **2012**, *9* (2), 73−74.
(27) Resnicow, D. I.; Deacon, J. C.; Warrick, H. M.; Spudich, J. A.; Leinwand, L. A. Functional diversity among a family of human skeletal muscle myosin motors. *Proc. Natl. Acad. Sci. U. S. A.* **2010**, *107* (3), 1053−1058.
(28) Sommese, R. F.; Sung, J.; Nag, S.; Sutton, S.; Deacon, J. C.; Choe, E.; Leinwand, L. A.; Ruppel, K.; Spudich, J. A. Molecular consequences of the R453C hypertrophic cardiomyopathy mutation on human β-cardiac myosin motor function. *Proc. Natl. Acad. Sci. U. S. A.* **2013**, *110* (31), 12607−12612.
(29) Nicolau, D. V.; Nicolau, D. V., Jr; Solana, G.; Hanson, K. L.; Filipponi, L.; Wang, L.; Lee, A. P. Molecular motors-based micro- and nano-biocomputation devices. *Microelectron. Eng.* **2006**, *83* (4−9SPEC. ISS.), 1582−1588.
(30) Korten, S.; Albet-Torres, N.; Paderi, F.; Ten Siethoff, L.; Diez, S.; Korten, T.; Te Kronnie, G.; Månsson, A. Sample solution constraints on motor-driven diagnostic nanodevices. *Lab Chip* **2013**, *13* (5), 866−876.
(31) Fulga, F.; Nicolau, D. V. Models of protein linear molecular motors for dynamic nanodevices. *Integr Biol.* **2009**, *1* (2), 150−169.
(32) Howard, J. *Mechanics of Motor Proteins and the Cytoskeleton*; Sinauer Associates, Inc.: Sunderland, MA, 2001.
(33) Albet-Torres, N.; O'Mahony, J.; Charlton, C.; Balaz, M.; Lisboa, P.; Aastrup, T.; Månsson, A.; Nicholls, I. A. Mode of heavy meromyosin adsorption and motor function correlated with surface hydrophobicity and charge. *Langmuir* **2007**, *23* (22), 11147−11156.
(34) Fischer, T.; Hess, H. Materials chemistry challenges in the design of hybrid bionanodevices: Supporting protein function within artificial environments. *J. Mater. Chem.* **2007**, *17* (10), 943−951.
(35) Sundberg, M.; Rosengren, J. P.; Bunk, R.; Lindahl, J.; Nicholls, I. A.; Tagerud, S.; Omling, P.; Montelius, L.; Mansson, A. Silanized surfaces for in vitro studies of actomyosin function and nano-technology applications. *Anal. Biochem.* **2003**, *323* (1), 127−138.
(36) Schneider, C. A.; Rasband, W. S.; Eliceiri, K. W. NIH Image to ImageJ: 25 years of image analysis. *Nat. Methods* **2012**, *9* (7), 671−675.
(37) Hase, M.; Yoshikawa, K. Structural transition of actin filament in a cell-sized water droplet with a phospholipid membrane. *J. Chem. Phys.* **2006**, *124*, (10).10490310.1063/1.2174004
(38) Hosek, M.; Tang, J. X. Polymer-induced bundling of F actin and the depletion force. *Phys. Rev. E* **2004**, *69*, (5).10.1103/PhysRevE.69.051907
(39) Rossi, R.; Maffei, M.; Bottinelli, R.; Canepari, M. Temperature dependence of speed of actin filaments propelled by slow and fast skeletal myosin isoforms. *J. Appl. Physiol.* **2005**, *99* (6), 2239−2245.
(40) Zechel, K.; Weber, K. Actins from mammals, bird, fish and slime mold characterized by isoelectric focusing in polyacrylamide gels. *Eur. J. Biochem.* **1978**, *89* (1), 105−112.
(41) Huxley, A. F. Muscle Structure and Theories of Contraction. *Prog. Biophys. Mol. Biol.* **1957**, *7*, 255.
(42) Pate, E.; White, H.; Cooke, R. Determination of the myosin step size from mechanical and kinetic data. *Proc. Natl. Acad. Sci. U. S. A.* **1993**, *90* (6), 2451−2455.
(43) Persson, M.; Bengtsson, E.; Ten Siethoff, L.; Månsson, A. Nonlinear cross-bridge elasticity and post-power-stroke events in fast skeletal muscle actomyosin. *Biophys. J.* **2013**, *105* (8), 1871−1881.
(44) Kim, D.; Herr, A. E., Protein immobilization techniques for microfluidic assays. *Biomicrofluidics* **2013**, *7*, (4). 04150110.1063/1.4816934
(45) Vasina, E. N.; Paszek, E.; Nicolau, D. V., Jr; Nicolau, D. V. The BAD project: Data mining, database and prediction of protein adsorption on surfaces. *Lab Chip* **2009**, *9* (7), 891−900.
(46) Nicolau, D. V.; Solana, G.; Kekic, M.; Fulga, F.; Mahanivong, C.; Wright, J.; dos Remedios, C. G. Surface Hydrophobicity Modulates the Operation of Actomyosin-Based Dynamic Nanodevices. *Langmuir* **2007**, *23* (21), 10846−10854.
(47) Van Zalinge, H.; Aveyard, J.; Hajne, J.; Persson, M.; Mansson, A.; Nicolau, D. V. Actin filament motility induced variation of resonance frequency and rigidity of polymer surfaces studied by quartz crystal microbalance. *Langmuir* **2012**, *28* (42), 15033−15037.
(48) Low, S. C.; Shaimi, R.; Thandaithabany, Y.; Lim, J. K.; Ahmad, A. L.; Ismail, A. Electrophoretic interactions between nitrocellulose membranes and proteins: Biointerface analysis and protein adhesion properties. *Colloids Surf., B* **2013**, *110*, 248−253.
(49) Homsher, E.; Wang, F.; Sellers, J. R. Factors affecting movement of F-actin filaments propelled by skeletal muscle heavy meromyosin. *American Journal of Physiology - Cell Physiology* **1992**, *262* (3 31−3), C714−C723.
(50) Balaz, M.; Sundberg, M.; Persson, M.; Kvassman, J.; Monsson, A. Effects of surface adsorption on catalytic activity of heavy meromyosin studied using a fluorescent ATP analogue. *Biochemistry* **2007**, *46* (24), 7233−7251.

DOI: 10.1021/acs.langmuir.5b01549
Langmuir 2015, 31, 8354−8361

(51) Spudich, J. A. How Molecular Motors Work. *Nature* **1994**, *372* (6506), 515−518.
(52) Sellers, J. R. In Vitro Motility Assay to Study Translocation of Actin by Myosin. *Current Protocols in Cell Biology*; John Wiley & Sons, Inc.: 2001.
(53) Warshaw, D. M. The in vitro motility assay: A window into the myosin molecular motor. *News in Physiological Sciences* **1996**, *11*, 1−7.
(54) Sundberg, M.; Balaz, M.; Bunk, R.; Rosengren-Holmberg, J. P.; Montelius, L.; Nicholls, I. A.; Omling, P.; Tagerud, S.; Mansson, A. Selective spatial localization of actomyosin motor function by chemical surface patterning. *Langmuir* **2006**, *22* (17), 7302−7312.
(55) Suzuki, H.; Yamada, A.; Oiwa, K.; Nakayama, H.; Mashiko, S. Control of actin moving trajectory by patterned poly-(methylmethacrylate) tracks. *Biophys. J.* **1997**, *72* (5), 1997−2001.
(56) Edman, K. A. P., The velocity of unloaded shortening and its relation to sarcomere length and isometric force in vertebrate muscle fibres. *J. Physiol.* **1979**, *291*, 143−159.10.1113/jphysiol.1979.sp012804
(57) Edman, K. A. P. The force-velocity relationship at negative loads (assisted shortening) studied in isolated, intact muscle fibres of the frog. *Acta Physiol.* **2014**, *211* (4), 609−616.
(58) Albet-Torres, N.; Gunnarsson, A.; Persson, M.; Balaz, M.; Hook, F.; Mansson, A. Molecular motors on lipid bilayers and silicon dioxide: different driving forces for adsorption. *Soft Matter* **2010**, *6* (14), 3211−3219.
(59) Kaya, M.; Higuchi, H. Nonlinear elasticity and an 8-nm working stroke of single myosin molecules in myofilaments. *Science* **2010**, *329* (5992), 686−689.

DOI: 10.1021/acs.langmuir.5b01549
Langmuir 2015, 31, 8354−8361